

Continuous Simultaneous Recording of Brachial Artery Distension and Wall Shear Rate: a New Boost for Flow-Mediated Vasodilation

Alessandro Ramalli, *Member, IEEE*, Kunihiro Aizawa, Angela C. Shore, Carmela Morizzo, Carlo Palombo, Matteo Lenge, Piero Tortoli, *Member, IEEE*

Abstract— Vascular ultrasound has been extensively applied in the clinical setting to noninvasively assess endothelial function by means of the so-called brachial artery flow mediated dilation (FMD). Despite the usefulness in large-scale epidemiological studies, this approach has revealed some pitfalls for assessing vascular physiology and health in individual subjects. Mainly, a reliable FMD examination should be based on the simultaneous and reliable measurement of both the stimulus, i.e. the wall shear rate (WSR), and the response, i.e. the diameter change. However, multiple technical, practical, and methodological challenges must be faced to meet this goal. In this work, we present the technical developments needed to implement a system to enable extensive and reliable clinical ultrasound FMD examination. It integrates both a hardware, i.e. an upgraded version of the ultrasound advanced open platform (ULA-OP), and a software part, i.e. a signal processing and data analysis platform. The system was applied for a two-center pilot clinical study on 35 young and healthy volunteers. Therefore, we present here the results of a statistical analysis on magnitude, time-course and kinetic parameters of WSR and diameter trends that allowed us to accurately explore the vasodilatory response to the dynamic wall shear rate changes. Our observations demonstrate that a direct and accurate estimation of WSR stimulus by multigate spectral Doppler allows understanding brachial artery vasodilatory response to reactive hyperemia. Drawing inferences on WSR stimulus from the diameter response along with an inaccurate estimation of WSR may cause further uncertainties for the accurate interpretation of the FMD response.

Index Terms— Real-time; Ultrasound system; Endothelial function; Reactive hyperemia; Vasodilation; Wall shear stress.

I. INTRODUCTION

Brachial artery flow-mediated dilation (FMD), a biomarker of endothelial function [1], consists of measuring the diameter

change of the brachial artery during the hyperemic “reactive” phase, induced by a transient arterial occlusion. During such reactive phase, the endothelial cells, activated by a sharp increase of the wall shear rate (WSR, i.e. the blood velocity gradient close to the walls), release nitric oxide (NO), a powerful vasodilator, thus inducing the dilation of the brachial artery. FMD has been extensively applied both in the clinical setting and the physiological research setting [2]–[9]: first, to determine a prognostic utility of FMD, e.g. in subjects with increased cardiovascular risks; then to identify the mechanisms that underlie the acute or chronic impact of stimuli that alter vascular function and risk.

Despite the usefulness in epidemiological studies, this approach has revealed some pitfalls for assessing vascular physiology and health in individual subjects. The main one is represented by the lack of a direct measurement of WSR during the maneuver. In the current routine application of FMD, WSR is estimated through the Doppler ultrasound peak velocity and the vessel diameter, assuming an ideal fully parabolic flow velocity profile [10]. However, this method frequently underestimates WSR [11] and is a blunt instrument to dissect the complex and dynamic WSR events occurring during FMD.

In the absence of reliable WSR data, the accurate interpretation of the FMD response may be confounded. A reduced FMD response might indicate either a relatively impaired endothelial function associated with reduced NO bioavailability, or it could also result from a reduced WSR increase in response to the stimulus with a preserved function of the endothelial cells. The reduced WSR increase, in turn, can be putatively attributed to vessel geometry, local stiffness or adrenergic vasoconstriction [12].

In order to translate the ultrasound FMD method to a widespread clinical tool that can be used in physiological

This work was supported by the NIHR Exeter Clinical Research Facility. The views of those of the authors and not necessarily those of UK National Institute of Health Research or the Department of Health.

A. Ramalli is with the Laboratory of Cardiovascular Imaging and Dynamics, Department of Cardiovascular Sciences, KU Leuven, 3000 Leuven, Belgium but he was with the Department of Information Engineering, University of Florence, 50139 Florence, Italy when part of the work was done. A. Ramalli has received funding from the European Union's Horizon 2020 research and innovation programme under the Marie Skłodowska-Curie grant agreement No 786027 (ACOUSTIC). (e-mail: alessandro.ramalli@kuleuven.be).

K. Aizawa and A. C. Shore are with the Diabetes and Vascular Medicine Research Centre, NIHR Exeter Clinical Research Facility, University of Exeter Medical School, EX2 5AX Exeter, UK.

C. Morizzo, C. Palombo are with the Department of Surgical, Medical, Molecular Pathology and Critical Care Medicine, University of Pisa, 56124 Pisa, Italy.

M. Lenge is with the Department of Neurosurgery and Department of Neuroscience, Meyer Children's Hospital and University of Florence, 50139 Florence, Italy.

P. Tortoli is with the Department of Information Engineering, University of Florence, 50139 Florence, Italy.

studies, the WSR-FMD stimulus-response relationship must be comprehensively characterized. First simultaneous measurements of both the WSR and the vessel diameter, made with single-element probes [13] or with short (5s) discontinuous acquisitions on a few healthy volunteers [14], highlighted technical, practical, and methodological challenges to be faced: a) the need of continuous recording for long acquisition times (up to 15 minutes); b) a real-time feedback that would allow an operator to monitor the long exam; c) an advanced set of post-processing tools to extract details from the analysis of WSR and diameter trends. Thus, we developed an ultrasound system, consisting of a hardware and a software part, capable of continuously processing and recording a huge amount of data (up to 16 GB); we developed processing algorithms to assess and monitor in real-time the flow velocity profile through the vessel as well as the diameter of the vessel [15], [16]. The new system was recently used in a small cohort study to establish a new benchmark in WSR-FMD measurement and to establish a normal reference of the WSR-FMD response [17]. In the current work, we first detail the hardware and software tools so far developed by our group. The focus is on the main processing algorithms and on the implemented hardware upgrades to allow continuous acquisitions for long exams (Sec. II). Descriptions of the volunteers' cohort and of the acquisition protocol are also given. Then, we characterize the stimulus-response relationship by conducting a statistical analysis on magnitude, time-course and kinetics parameters of WSR/diameter trends obtained through a two-center (Exeter and Pisa) pilot clinical study on 35 healthy young volunteers. Section III shows results of the analysis that are finally discussed in section IV.

II. MATERIALS AND METHODS

A. Hardware: the ULA-OP

The ULA-OP [18], acronym for ultrasound advanced open platform, is a complete ultrasound system for research & development and was fully designed at the Microelectronics Systems Design Laboratory (Department of Information Engineering, University of Florence, Italy). The system, through 64 independent channels in both transmission and reception (TX and RX), controls linear/convex/phased array probes with up to 192 transducers by a programmable multiplexer. The system consists of two main processing boards: the analog board and the digital board. The former contains the front-end electronics for analog conditioning of the 64 channels and the multiplexer; the latter board manages, through five Field Programmable Gate Arrays (FPGAs) and one Digital Signal Processor (DSP), the synthesis of the transmission patterns, the real-time beamforming, the quadrature demodulation and the signal processing. The ULA-OP communicates through a USB 2.0 channel with a host PC, equipped with a specific real-time software tool providing the real-time visualization of ultrasound images, processed in various modes.


The ULA-OP system offers full access to the signal data collected at each step of the processing chain. Since an FMD

exam lasts up to 15 minutes, a dedicated additional acquisition board has been developed to store the demodulated quadrature data over such a long time. This board includes a 16 GB compact flash memory card, and also allows acquiring auxiliary signals such as those produced by an ECG device or a tonometer [16].

B. Real-time firmware/software

The ULA-OP was programmed in duplex mode by interleaving the transmission sequences for the B-mode and the Multi-gate Spectral Doppler (MSD) mode, so that the mode is alternated between pairs of sequential transmissions.

The firmware running on the DSP that is onboard the ULA-OP, processes the quadrature demodulated data: it performs 2D filtering and logarithmic compression for B-mode data; while it computes the 256-point Fast Fourier Transform (FFT) for each sample volume along the Doppler investigation line and extracts the complex envelope to generate the MSD profile [19]–[21].

The software running on the PC manages the real-time display that, for the purpose of this work, was split into 3 panels, as shown in Fig. 1 and in the accompanying clip : the top-left panel shows the B-mode image with the Doppler investigation line; the top-right panel shows the MSD profile; and the bottom panel shows the diameter time-trend of the vessel under exam. The real-time display of both MSD profiles and diameter trends is very important to prevent or correct possible probe-to-arm movements that may happen during long exams, thus jeopardizing the final analysis of the results. Indeed, the diameter estimation is very sensitive and is able to detect diameter changes in the order of tens of microns during the cardiac cycle; hence, when small, unexpected probe-to-arm movements happen, they are barely visible on the B-mode image, but determine a sudden, well visible, change in the diameter trend. Accordingly, the operator can choose whether trying to replace the probe or restarting the examination.

In particular, the diameter is estimated in real-time by means of a modified version [16] of the algorithm proposed in [22] that exploits an edge-detection algorithm. It is initialized as follows:

1. the operator selects, on any B-mode frame, one point inside the vessel lumen;
2. the software automatically generates two 8mm-long segments, one placed shallower and the other one deeper than the initialization point;
3. 16 equidistant points are automatically selected on each segment.

Hence, the module processes each B-mode grayscale frame as follows:

- 4a. for each of the 16 points along a search-segment, in a circular domain of about 1.2 mm radius the mass center of the first order absolute central moment (FOAM) of the gray-level function is computed [22], [23];
- 4b. the position of each point is associated with the position of the mass center;

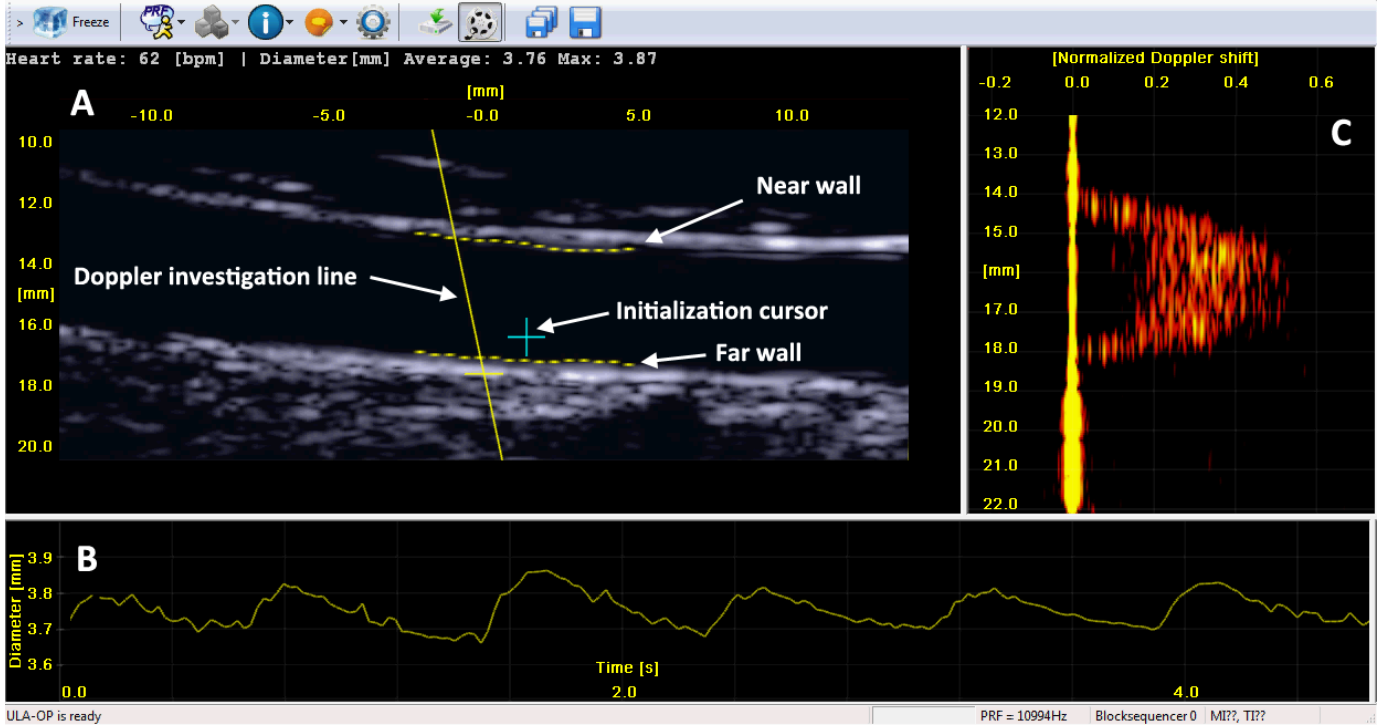


Fig. 1 The ULA-OP software interface during an exam on the brachial artery of a healthy volunteer. The interface shows in real-time: (A) the B-mode images, including the near and far wall markers (dotted yellow lines) calculated by the edge-detection algorithm; the diameter trend (B); and (C) the multi-gate spectral Doppler profile (with depth on vertical axis, Doppler shifts on horizontal axis and local power spectral Doppler densities modulating the pixel intensities), obtained along the Doppler investigation line (solid yellow line in panel A).

4c. the evaluation iteratively proceeds until the point converges to the wall of the vessel. Specifically, the point is considered converged to the wall when its position change on two consecutive iterations is smaller than $30 \mu\text{m}$. Typically, the condition is achieved in less than 5 iterations; anyway, an upper limit to the number of iterations is set to 10.

In the end, the position of the two sets of points corresponds to the instantaneous position of the far and near walls of the vessel (dotted yellow lines in Fig.1A); the average distance between the two walls is assumed as the instantaneous diameter.

C. Post-processing software

A Matlab® based software platform was developed to describe, through multiple parameters, the time-course and the amplitude of changes in the WSR and in the vessel diameter. The platform processes the acquired files containing quadrature demodulated signals emulating the processing chain of the ULA-OP system: accordingly, it computes the B-mode images (Fig. 2 panel A), returns the instantaneous position of the walls and the diameter (Fig. 2 panel E), and extracts the MSD profiles (Fig. 2 panel B). In addition, the MSD profiles are further processed to estimate the blood flow speed (Fig. 2 panel C) and the instantaneous WSR (Fig. 2 panel D) according to the algorithm introduced in [13], suitably modified to exploit the knowledge of the position of the vessel walls extracted from B-mode images [24]. In detail, for each instantaneous MSD profile obtained along the Doppler investigation line, the WSR processing module:

1. Filters the clutter through a high-pass mask in the Doppler

frequency domain;

2. Computes the power-weighted mean frequency f_D for each depth d and converts it to flow speed through the Doppler equation:

$$v(d) = (c \cdot f_D(d)) / (2f_0 \cdot \cos\theta_D) \quad (1)$$

where f_0 is the transmitted central frequency, c is the speed of sound, and θ_D is the Doppler angle. The latter is estimated as the angle between the Doppler investigation line and the linearized wall directions extrapolated from the diameter extraction module.

3. Fits $v(d)$ with a polynomial least-square fitting;

4. Evaluates the shear rate (SR), i.e. the gradient of the fit curve with respect to the vessel radius (r);

$$SR(r) = dv/dr \quad (2)$$

5. Estimates the near and far WSR as the peak shear rates close to the near and far walls, respectively.

$$WSR = \max[SR(r)|_{R-0.5\text{mm} < r < R+0.5\text{mm}}] \quad (3)$$

where R is the estimated radius of the vessel.

Finally, both instantaneous WSR (Fig. 2 panel D) and diameter (Fig. 2 panel E) trends are saved in a file.

D. Definition of estimated parameters

The saved files are further processed by an analysis interface, shown in Fig. 3, that allows the extraction of detailed WSR and diameter parameters to describe magnitude, kinetics and time-course of their changes. As sketched in Fig. 3 (top), the following WSR magnitude parameters and WSR kinetics

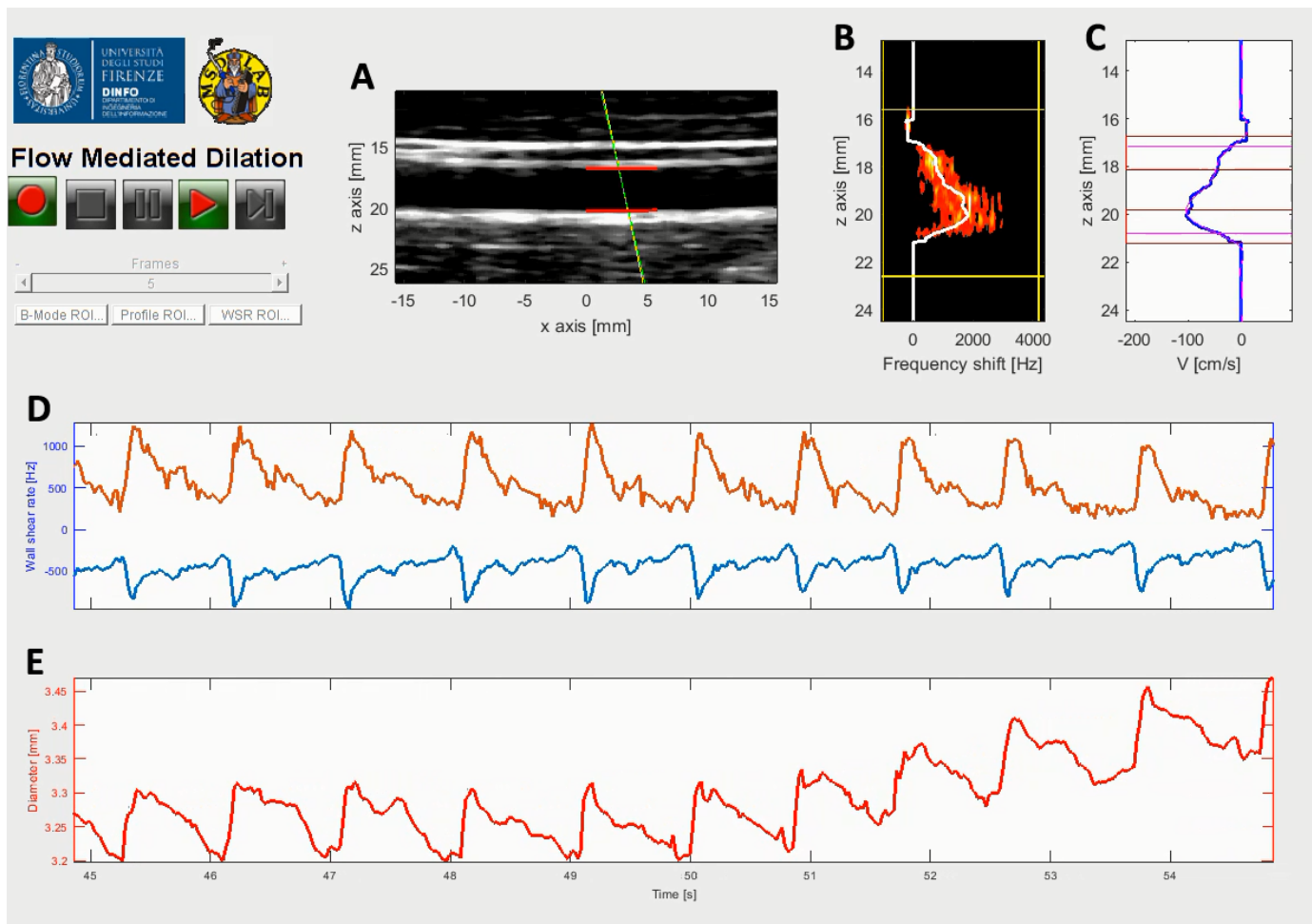


Fig. 2 Graphical user interface of the Matlab based software platform. (A) B-mode image; (B) MSD profiles; (C) blood flow speed; (D) instantaneous WSR of near (light blue) and far (orange) walls; (E) instantaneous diameter. (B) and (C) highlight the asymmetry of the flow profile with respect to the vessel center: different WSR values are detected for near and far wall as shown in (D). The graphical user interface was captured after 50 s from the beginning of the acquisition, i.e. 20 s after the release; at this time the WSR is already decreasing (D), while the diameter begins to increase (E).

The processing of part of the acquisition is shown in the accompanying clip [\[1\]](#): it starts 5 s before the cuff release and lasts 100 s. The clip shows: the release (00:05), the WSR peak (roughly 00:16), the beginning of the diameter increase (roughly 00:24), the return to baseline values of the WSR (roughly 01:02), the diameter peak (roughly 01:12 s) and the decreasing phase of the diameter (until the end of the clip).

parameters were estimated:

- WSR average value at baseline (WSR Baseline);
- WSR at peak hyperemia (WSR Peak);
- Absolute WSR increase from baseline (WSR Δ);
- Percent WSR increase from baseline (WSR % Δ);
- Area under the WSR curve until time to peak dilation of the diameter (WSR Aucttp);
- Area under the WSR curve (WSR Auc), measured between cuff release and the point at which WSR returned to the baseline value;
- First slope of WSR increase during hyperemia (WSR SL1, an initial steep increase);
- The second slope of WSR increase during hyperemia (WSR SL2, a gradual increase after the initial steep increase; when observed).

Similarly, as sketched in Fig. 3 bottom, 2 diameter magnitudes and 2 diameter time-course parameters were estimated:

- Diameter average value at baseline (Diameter Baseline);

- Absolute diameter increase from baseline (Diameter Δ);
 - Percent diameter increase from baseline (Diameter % Δ);
 - Time from cuff release to peak diameter (Diameter Tp);
 - Time to return to baseline diameter, taken as the point at which diameter returns to its baseline values (Diameter Tb).
- In this study, 3 diameter kinetics parameters were analyzed:
- The first slope of diameter increase after cuff-deflation (DIAM SL1, an initial steep diameter increase);
 - The second slope of diameter increase (DIAM SL2, a gradual diameter increase after the initial steep increase when observed);
 - The diameter decrease slope (DIAM SL3, a diameter decrease after reaching its peak value).

Data are presented as mean \pm standard deviation, median (interquartile ranges) or numbers. A partial correlation analysis was performed between diameter kinetics parameters, diameter change parameters and diameter time-course parameters controlling for the study center. A partial correlation analysis

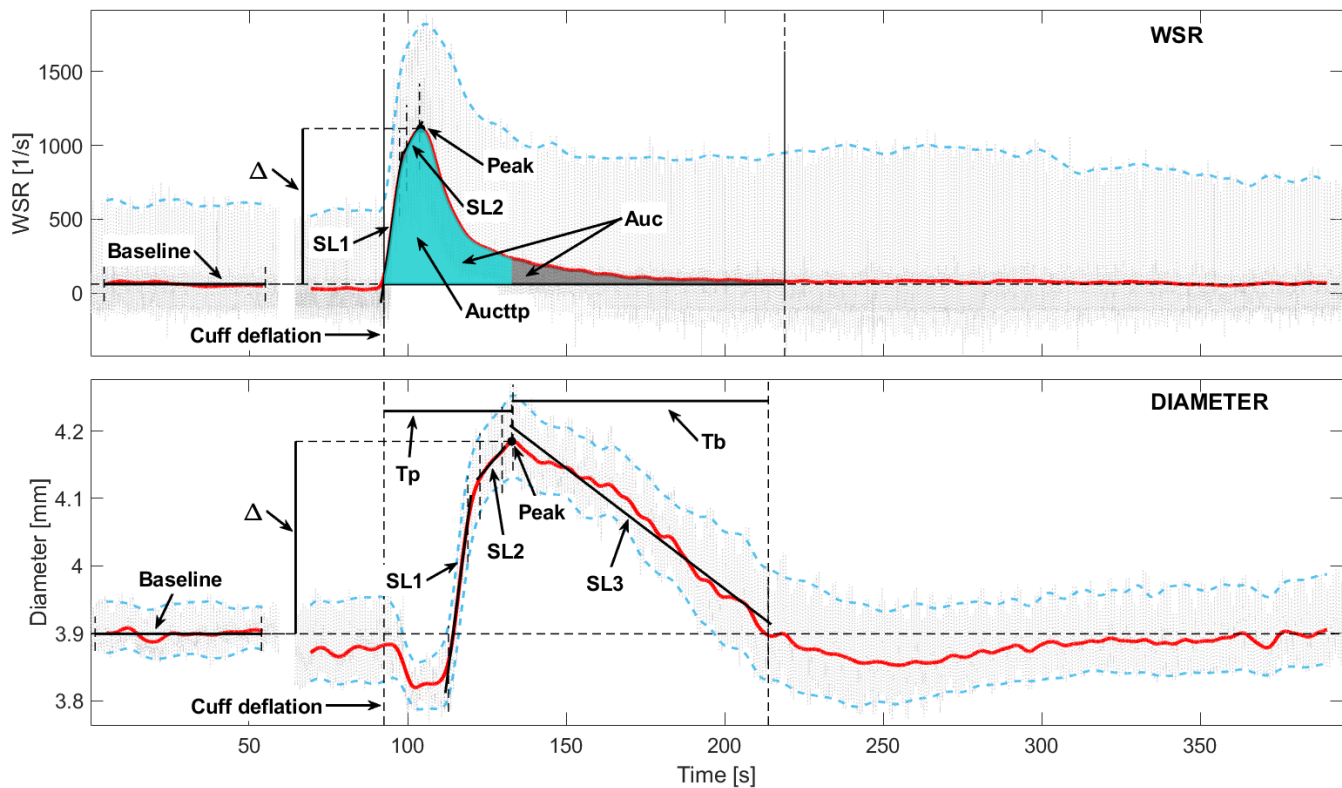


Fig. 3 A schematic description of wall shear rate (WSR) and diameter parameters obtained from brachial artery flow-mediated dilation (FMD). Top: traces in light blue and red represent the peak and mean values of WSR, respectively. Bottom: traces in light blue and red represent the variations in diameter (due to cardiac cycle) and mean diameter of the brachial artery, respectively. Please, refer to section II D for the definition of the parameters and their abbreviations.

was also performed between diameter kinetics parameters and WSR parameters controlling for the study center. A log transformation was used for variables with skewed distribution before statistical analysis. Statistical significance was set at $p < 0.05$ and all statistical analysis was performed using IBM SPSS Statistics 24 (IBM, Armonk, NY).

E. Participants

Thirty-five participants were included in this study. Of these, 17 were recruited in Exeter, UK and 18 in Pisa, Italy. All participants were young (defined as $20 \leq \text{age} < 40$ yrs) healthy adults without the presence of hypertension, type 2 diabetes, dyslipidaemia or overt cardiovascular disease. No one took any medications for cardiovascular risk modifications. Selected characteristics of the study participants are shown in TABLE I. All study procedures were approved by UK National Research Ethics Service South West Committee and the institutional ethics committee at University of Pisa. All participants provided written informed consent before being included in the study.

F. Protocol

All the procedures were conducted in our temperature-controlled laboratories. Participants arrived at the laboratories after an overnight fast, had blood samples taken for biochemical analysis, consumed a standardized meal and then rested for 20 min before the initiation of the study protocol.

The details of our brachial artery FMD assessment, which is kept in accordance with established guidelines [25]–[27], are

described in [17], [28]. Briefly, participants lay supine on an examination bed with the right arm fixed in position and immobilized using a positioning pillow on a metal table. A small blood pressure cuff was positioned around the proximal part of the forearm to create a temporal forearm ischemia. As described above, B-mode ultrasound images and MSD data from the brachial artery were obtained using the ULA-OP connected to a 9-MHz linear array probe (LA523; Esaote SpA, Florence, Italy). The probe was clamped once the optimal B-mode image was obtained using a custom-designed probe holder to prevent movement during the procedure. Raw baseband data, producing baseline brachial artery image and multi-gate Doppler velocity, were recorded for 60 s, after which the cuff was rapidly inflated to 250 mmHg to occlude forearm blood flow for 5 min using a commercially available arterial inflow system (AI6, Hokanson, Bellevue, WA). Thirty seconds before deflation, recording was restarted and continued for 5 min following deflation.

TABLE I
SELECTED CHARACTERISTICS OF THE STUDY PARTICIPANTS

Age [yrs]	27.2±5.0
Number of female/male	21/14
Body mass index [kg/m ²]	22.7±3.0
Systolic blood pressure [mmHg]	113.9±10.1
Diastolic blood pressure [mmHg]	68.7±6.7
Heart rate [bpm]	64.0±10.0

III. RESULTS

The parameters of WSR (magnitude and kinetics) and diameter (magnitude, time-course and kinetics) obtained during the brachial artery FMD assessment from our healthy young participants are summarized in TABLE II. The magnitude of diameter changes observed in this study (6.6%) was similar to what healthy young individuals typically exhibited during brachial artery FMD assessment (for example 7.3% in [29]), while WSR cannot be fairly compared since, as demonstrated in [14], WSR was so far frequently underestimated.

TABLE III and Fig. 4 A-B show the results of partial correlation analysis between diameter kinetics parameters and diameter magnitude parameters in this study. DIAM SL1 was significantly associated with both absolute and percentage diameter changes (both $p < 0.05$). However, DIAM SL2 did not associate with diameter magnitude parameters. A lack of association was also observed between DIAM SL3 and diameter magnitude parameters.

TABLE III and Fig. 4 C-D show the results of partial correlation analysis between diameter kinetics parameters and diameter time-course parameters in this study. A significant inverse association was observed between DIAM SL1 and the time to peak diameter ($p < 0.05$). This was also the case between DIAM SL2 and the time to peak diameter ($p < 0.05$). DIAM SL3 was not associated with the time to peak diameter. DIAM SL3 was significantly associated with the time to return to baseline diameter ($p < 0.05$), which was not the case for DIAM SL1 or DIAM SL2.

The results of partial correlation analysis between diameter kinetics parameters and WSR parameters are shown in TABLE IV. None of diameter kinetics parameters showed any association with WSR magnitude parameters. A lack of association was also observed between diameter kinetics parameters and WSR kinetics parameters. These observations remained unchanged when WSR parameters derived from peak values were used for analysis (data not shown).

IV. DISCUSSION AND CONCLUSION

This paper has presented a system that enables extensive clinical ultrasound FMD examinations based on the simultaneous and reliable measurement of both the stimulus

TABLE III
PARTIAL CORRELATION ANALYSIS BETWEEN DIAMETER KINETICS, MAGNITUDE AND TIME-COURSE PARAMETERS OF THE STUDY PARTICIPANTS.

	DIAM SL1	DIAM SL2 †	DIAM SL3
Diameter Magnitude Parameters			
Diameter Δ	$r=0.417$, $p=0.014$	$r=0.024$, $p=0.920$	$r=-0.079$, $p=0.662$
Diameter %Δ	$r=0.374$, $p=0.029$	$r=0.044$, $p=0.853$	$r=-0.062$, $p=0.731$
Diameter Time-Course Parameters			
Diameter Tp	$r=-0.381$, $p=0.026$	$r=-0.461$, $p=0.041$	$r=-0.030$, $p=0.868$
Diameter Tb	$r=0.166$, $p=0.348$	$r=0.245$, $p=0.298$	$r=0.356$, $p=0.042$

†Obtained from 21 participants who showed a 2nd diameter increase response.

TABLE II
PARAMETERS OF WALL SHEAR RATE AND DIAMETER DURING THE BRACHIAL ARTERY FLOW-MEDIATED DILATION ASSESSMENT IN A HEALTHY YOUNG COHORT.

WSR Magnitude Parameters	
WSR baseline [1/s]	100.8±54.9
WSR peak [1/s]	587.3±156.7
WSR Δ [1/s]	486.5±157.0
WSR %Δ	590.1% (269.6% - 967.9%)
WSR aucttp [au]	15150±5943
WSR auc [au]	17110±6625
WSR Kinetics Parameters	
WSR SL1 [1/s²]	79.3±26.6
WSR SL2, [1/s²] *	16.4±8.8
Diameter Magnitude Parameters	
Diameter baseline [mm]	3.28±0.44
Diameter Δ [mm]	0.21±0.10
Diameter %Δ	6.6%±3.4%
Diameter Time-Course Parameters	
Diameter Tp [s]	54.8±30.5
Diameter Tb [s]	114.5±58.8
Diameter Kinetics Parameters	
DIAM SL1 [mm/s]	0.018±0.010
DIAM SL2 [mm/s] †	0.005±0.004
DIAM SL3 [mm/s]	-0.002±0.003

*Obtained from 18 participants who showed a 2nd WSR increase response.
†Obtained from 21 participants who showed a 2nd diameter increase response.

(WSR change) and the response (diameter change). The system, which integrates both a hardware, i.e. an upgraded version of the ULA-OP system, and a software part, i.e. a signal processing and data analysis platform developed in Matlab, has been used in a two-center (Exeter and Pisa) pilot clinical study

TABLE IV
PARTIAL CORRELATION ANALYSIS BETWEEN DIAMETER KINETICS PARAMETERS AND WSR PARAMETERS OF THE STUDY PARTICIPANTS.

	DIAM SL1	DIAM SL2 †	DIAM SL3
WSR Magnitude Parameters			
WSR peak	$r=0.220$, $p=0.210$	$r=0.094$, $p=0.692$	$r=-0.198$, $p=0.270$
WSR Δ	$r=0.133$, $p=0.453$	$r=0.113$, $p=0.634$	$r=-0.174$, $p=0.334$
WSR %Δ	$r=-0.165$, $p=0.351$	$r=0.010$, $p=0.966$	$r=0.045$, $p=0.801$
WSR Aucttp	$r=-0.169$, $p=0.338$	$r=0.013$, $p=0.955$	$r=-0.224$, $p=0.210$
WSR Auc	$r=-0.143$, $p=0.420$	$r=0.081$, $p=0.735$	$r=-0.193$, $p=0.282$
WSR Kinetics Parameters			
WSR SL1	$r=0.138$, $p=0.436$	$r=0.083$, $p=0.729$	$r=-0.090$, $p=0.620$
WSR SL2 *	$r=0.061$, $p=0.816$	$r=0.086$, $p=0.781$	$r=-0.288$, $p=0.262$

*Obtained from 18 participants who showed a 2nd WSR increase response.
†Obtained from 21 participants who showed a 2nd diameter increase response.

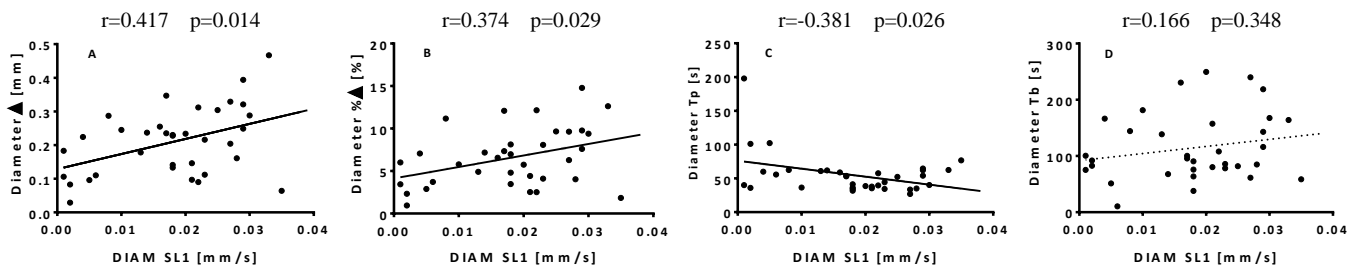


Fig. 4 Univariate correlation analysis between DIAM SL1 and diameter magnitude parameters (A and B), and between DIAM SL1 and diameter time-course parameters (C and D) in the study participants. Δ , absolute change; $\% \Delta$, percentage change; DIAM SL1, the first slope of the diameter increase after cuff-deflation; Tp, time to peak dilation; Tb, time to return to baseline.

on 35 young and healthy volunteers.

The system was able to overcome multiple technical, practical, or methodological challenges emerged from previous studies [14]–[16]:

1. The ULA-OP scanner was upgraded with a purposely designed board providing extended memory capabilities. Up to 16 GB of quadrature demodulated data can now be acquired on a compact flash memory card, ensuring the continuous acquisition of both B-mode and MSD data for examinations lasting up to 15 minutes, e.g. FMD examinations. In previous studies [14], to limit the amount of data storage, the acquisition was made in slots of 4 s spaced apart 5/10 s, thus limiting the time-resolution of WSR and diameter trends. Detailed and prolonged information about the WSR stimulus and FMD response are generated, opening new perspectives for the investigation of endothelial function in humans.
2. The real-time software was upgraded with a processing module that allows showing the diameter trend together with the MSD profiles. Now, by monitoring the real-time display Fig. 1, the operator can quickly find the optimal probe position through the availability of MSD profiles, while he/she can control the stability of the probe orientation, and promptly correct for possible small probe-to-arm movements [16], through the B-mode and the diameter trend changes. Previously, with the B-mode only, the operator could not detect such small movements until after the processing of the whole acquisition, making it necessary to repeat the whole examination in the case of previously undetected probe-to-arm movements.
3. Until now, in a clinical setting, WSR was assessed considering the (often misleading) assumption of parabolic (symmetric) flow profile [13], [14], [17], [20], [30]; in this work, the implementation of MSD on both the ULA-OP scanner and on the signal elaboration platform, allowed the independent estimation of the WSR close to the arterial wall without any assumption on the flow profile. In addition, the availability of wall directions, extrapolated from the diameter extraction module, allows an objective estimation of the Doppler angle and hence a more reliable flow speed estimation when compared to standard clinical systems, where the flow direction is roughly and subjectively set by the user.
4. The developed software interface (Fig. 2 and Fig. 3) allowed estimation of several magnitude, time-course, and kinetic

parameters from the time trends of both WSR and diameter that could not be assessed before [15] and that may enable better understanding of vascular physiology and pathology.

The main findings of this study are that, in a young healthy population, the slope of the first diameter increase (DIAM SL1) was associated with the brachial artery vasodilatory response during the FMD assessment. The first and second slopes of the diameter increase (DIAM SL1 and DIAM SL2) were also inversely associated with the time to peak diameter. The diameter deceleration slope (DIAM SL3) was positively associated with the time to return to baseline diameter. In contrast, diameter kinetics parameters were not associated with WSR magnitude parameters nor with WSR kinetics parameters. These findings suggest that diameter kinetics parameters derived from a diameter change curve predict the magnitude and time-course of a vasodilatory ‘response’ during the brachial artery FMD assessment in the young. However, these diameter kinetics parameters may be insufficient to determine the magnitude, as well as the kinetics, of WSR ‘stimulus’ occurring during reactive hyperemia in this cohort. Our observations clearly demonstrate that a direct and accurate estimation of WSR stimulus by MSD is imperative to understand brachial artery vasodilatory response to reactive hyperemia. Drawing inferences on WSR stimulus from the diameter response along with an inaccurate estimation of WSR may cause further uncertainties for the accurate interpretation of the FMD response.

Although experienced operators performed all FMD assessments, an important limitation of this pilot clinical study is the lack of reproducibility measurements, e.g. after probe repositioning or with different operators, addressed to understand the sources of variability in this delicate measurement. Moreover, possible extensions of this work might be related to the exploitation of 3D imaging approaches that might improve the robustness of the diameter estimation to probe-to-arm movements; at the same time 3D vector Doppler [31]–[33] would improve the accuracy of the flow speed estimation (hence of the WSR) without making any assumption on the direction of the blood flow. Nevertheless, in straight vessels like the brachial artery, assuming the orientation of velocity vector to be parallel to the walls can be considered acceptable, 3D techniques with adequately high temporal resolution are still not easily implemented in real-time.

The FMD examination, which has so far been considered a

method with great potential but with limited application due to multiple practical difficulties, is finally close to clinical acceptance and applicability.

REFERENCES

- [1] Deanfield John E., Halcox Julian P., and Rabelink Ton J., "Endothelial Function and Dysfunction: Testing and Clinical Relevance," *Circulation*, vol. 115, no. 10, pp. 1285–1295, Mar. 2007.
- [2] D. S. Celermajer *et al.*, "Non-invasive detection of endothelial dysfunction in children and adults at risk of atherosclerosis," *The Lancet*, vol. 340, no. 8828, pp. 1111–1115, Nov. 1992.
- [3] D. S. Celermajer, K. E. Sorensen, C. Bull, J. Robinson, and J. E. Deanfield, "Endothelium-dependent dilation in the systemic arteries of asymptomatic subjects relates to coronary risk factors and their interaction," *J. Am. Coll. Cardiol.*, vol. 24, no. 6, pp. 1468–1474, Nov. 1994.
- [4] K. E. Pyke, E. M. Dwyer, and M. E. Tschakovsky, "Impact of controlling shear rate on flow-mediated dilation responses in the brachial artery of humans," *J. Appl. Physiol.*, vol. 97, no. 2, pp. 499–508, Aug. 2004.
- [5] K. E. Pyke and M. E. Tschakovsky, "Peak vs. total reactive hyperemia: which determines the magnitude of flow-mediated dilation?," *J. Appl. Physiol.*, vol. 102, no. 4, pp. 1510–1519, Apr. 2007.
- [6] J. Yeboah, J. R. Crouse, F.-C. Hsu, G. L. Burke, and D. M. Herrington, "Brachial Flow-Mediated Dilation Predicts Incident Cardiovascular Events in Older Adults: The Cardiovascular Health Study," *Circulation*, vol. 115, no. 18, pp. 2390–2397, May 2007.
- [7] J. Padilla *et al.*, "Adjusting Flow-Mediated Dilation for Shear Stress Stimulus Allows Demonstration of Endothelial Dysfunction in a Population with Moderate Cardiovascular Risk," *J. Vasc. Res.*, vol. 46, no. 6, pp. 592–600, 2009.
- [8] D. H. J. Thijssen *et al.*, "Does arterial shear explain the magnitude of flow-mediated dilation?: a comparison between young and older humans," *Am. J. Physiol.-Heart Circ. Physiol.*, vol. 296, no. 1, pp. H57–H64, Jan. 2009.
- [9] J. Yeboah *et al.*, "Predictive Value of Brachial Flow-Mediated Dilation for Incident Cardiovascular Events in a Population-Based Study: The Multi-Ethnic Study of Atherosclerosis," *Circulation*, vol. 120, no. 6, pp. 502–509, Aug. 2009.
- [10] A. Gnasso *et al.*, "Association between wall shear stress and flow-mediated vasodilation in healthy men," *Atherosclerosis*, vol. 156, no. 1, pp. 171–176, May 2001.
- [11] H. A. Silber, P. Ouyang, D. A. Bluemke, S. N. Gupta, T. K. Foo, and J. A. C. Lima, "Why is flow-mediated dilation dependent on arterial size? Assessment of the shear stimulus using phase-contrast magnetic resonance imaging," *Am. J. Physiol.-Heart Circ. Physiol.*, vol. 288, no. 2, pp. H822–H828, Feb. 2005.
- [12] K. E. Pyke, J. A. Hartnett, and M. E. Tschakovsky, "Are the dynamic response characteristics of brachial artery flow-mediated dilation sensitive to the magnitude of increase in shear stimulus?," *J. Appl. Physiol. Bethesda Md* 1985, vol. 105, no. 1, pp. 282–292, Jul. 2008.
- [13] P. Tortoli, T. Morganti, G. Bambi, C. Palombo, and K. V. Ramnarine, "Noninvasive simultaneous assessment of wall shear rate and wall distension in carotid arteries," *Ultrasound Med. Biol.*, vol. 32, no. 11, pp. 1661–1670, Nov. 2006.
- [14] P. Tortoli, C. Palombo, L. Ghiadoni, G. Bini, and L. Francalanci, "Simultaneous ultrasound assessment of brachial artery shear stimulus and flow-mediated dilation during reactive hyperemia," *Ultrasound Med. Biol.*, vol. 37, no. 10, pp. 1561–1570, Oct. 2011.
- [15] A. Ramalli, L. Bassi, M. Lenge, C. Palombo, K. Aizawa, and P. Tortoli, "An integrated system for the evaluation of flow Mediated Dilation," in *2014 IEEE International Conference on Acoustics, Speech and Signal Processing (ICASSP)*, 2014, pp. 5145–5148.
- [16] A. Ramalli *et al.*, "A multiparametric approach integrating vessel diameter, wall shear rate and physiologic signals for optimized Flow Mediated Dilation studies," in *Ultrasonics Symposium (IUS), 2015 IEEE International*, 2015.
- [17] K. Aizawa *et al.*, "Brachial artery vasodilatory response and wall shear rate determined by multigate Doppler in a healthy young cohort," *J. Appl. Physiol.*, vol. 124, no. 1, pp. 150–159, Nov. 2017.
- [18] E. Boni *et al.*, "A reconfigurable and programmable FPGA-based system for nonstandard ultrasound methods," *IEEE Trans. Ultrason. Ferroelectr. Freq. Control*, vol. 59, no. 7, pp. 1378–1385, Jul. 2012.
- [19] P. Tortoli, G. Guidi, P. Berti, F. Guidi, and D. Righi, "An FFT-based flow profiler for high-resolution in vivo investigations," *Ultrasound Med. Biol.*, vol. 23, no. 6, pp. 899–910, 1997.
- [20] P. Tortoli, G. Bambi, F. Guidi, and R. Muchada, "Toward a better quantitative measurement of aortic flow," *Ultrasound Med. Biol.*, vol. 28, no. 2, pp. 249–257, Feb. 2002.
- [21] A. Nowicki *et al.*, "20-MHz Ultrasound for Measurements of Flow-Mediated Dilation and Shear Rate in the Radial Artery," *Ultrasound Med. Biol.*, vol. 44, no. 6, pp. 1187–1197, Jun. 2018.
- [22] M. Demi, M. Paterni, and A. Benassi, "The First Absolute Central Moment in Low-Level Image Processing," *Comput. Vis. Image Underst.*, vol. 80, no. 1, pp. 57–87, Oct. 2000.
- [23] V. Gemignani, F. Fata, L. Ghiadoni, E. Poggianti, and M. Demi, "A System for Real-Time Measurement of the Brachial Artery Diameter in B-Mode Ultrasound Images," *IEEE Trans. Med. Imaging*, vol. 26, no. 3, pp. 393–404, Mar. 2007.
- [24] S. Ricci, A. Swillens, A. Ramalli, P. Segers, and P. Tortoli, "Wall Shear Rate Measurement: Validation of a New Method Through Multiphysics Simulations," *IEEE Trans. Ultrason. Ferroelectr. Freq. Control*, vol. 64, no. 1, pp. 66–77, Jan. 2017.
- [25] M. C. Corretti *et al.*, "Guidelines for the ultrasound assessment of endothelial-dependent flow-mediated vasodilation of the brachial artery: A report of the International Brachial Artery Reactivity Task Force," *J. Am. Coll. Cardiol.*, vol. 39, no. 2, pp. 257–265, Jan. 2002.
- [26] R. A. Harris, S. K. Nishiyama, D. W. Wray, and R. S. Richardson, "Ultrasound assessment of flow-mediated dilation: a tutorial," *Hypertension*, vol. 55, no. 5, pp. 1075–1085, May 2010.
- [27] D. H. J. Thijssen *et al.*, "Assessment of flow-mediated dilation in humans: a methodological and physiological guideline," *Am. J. Physiol.-Heart Circ. Physiol.*, vol. 300, no. 1, pp. H2–H12, Oct. 2010.
- [28] K. Aizawa *et al.*, "Reactivity to low-flow as a potential determinant for brachial artery flow-mediated vasodilatation," *Physiol. Rep.*, vol. 4, no. 12, p. e12808, Jun. 2016.
- [29] A. E. Donald *et al.*, "Non-Invasive Assessment of Endothelial Function: Which Technique?," *J. Am. Coll. Cardiol.*, vol. 48, no. 9, pp. 1846–1850, Nov. 2006.
- [30] L. Stoner, M. J. Sabatier, and J. M. Young, "Examination of Possible Flow Turbulence during Flow-Mediated Dilation Testing," *Open J. Med. Imaging*, vol. 01, no. 01, p. 1, Sep. 2011.
- [31] J. A. Jensen, S. I. Nikolov, A. C. H. Yu, and D. Garcia, "Ultrasound Vector Flow Imaging - Part I: Sequential Systems," *IEEE Trans. Ultrason. Ferroelectr. Freq. Control*, vol. 63, no. 11, pp. 1704–1721, Nov. 2016.
- [32] J. A. Jensen, S. I. Nikolov, A. C. H. Yu, and D. Garcia, "Ultrasound Vector Flow Imaging - Part II: Parallel Systems," *IEEE Trans. Ultrason. Ferroelectr. Freq. Control*, vol. 63, no. 11, pp. 1722–1732, Nov. 2016.
- [33] P. Tortoli, M. Lenge, D. Righi, G. Ciuti, H. Liebgott, and S. Ricci, "Comparison of carotid artery blood velocity measurements by vector and standard Doppler approaches," *Ultrasound Med. Biol.*, vol. 41, no. 5, pp. 1354–1362, May 2015.